

Identification of missense mutations in genes related to cancer pathways in glioma

¹Nor Azian Abdul Murad, ¹Saiful Effendi Syafruddin, ¹Muhiddin Ishak, ¹Mohd Ridhwan Abdul Razak, ¹Sri Noraima Othman, ^{1,2}Soon Bee Hong, ²Azizi Abu Bakar, ²Farizal Fadzil, ²Jegan Thanabalan, ²Toh Charng Jeng, ³Isa Mohamed Rose, ^{1,4}Roslan Harun, ¹Rahman Jamal

¹UKM Medical Molecular Biology Institute (UMBI); ²Department of Surgery, Faculty of Medicine; ³Department of Pathology, Faculty of Medicine; ⁴Department of Medicine, Faculty of Medicine, UKM, Cheras, Kuala Lumpur, Malaysia

Received on 15/03/2015 / Accepted on 08/09/2015

Abstract

Glioma is the most common primary brain tumour of the central nervous system. Many genetic alterations and mutations have been identified in glioma using various approaches. We performed DNA sequencing on the tumours of 16 patients with Grade I, II, III and IV glioma. The AmpliSeq Cancer Primers Pool was used to generate the amplicons. The targeted-ion sphere particles were prepared using the Ion One Touch and Ion Enrichment systems. DNA sequencing was performed on the Ion Torrent Personal Genome Machine (PGM) and the data were analysed using the Torrent Suite Software.

In total, 14 mutations were identified in the following genes: *KDR* (Q472H), *MLH1* (V384D), *MET* (N375S), *PTPN11* (E69K), *BRAF* (V600E), *TP53* (D149E, E154K, V157F), *IDH1* (R132H), *PIK3CA* (H1047R), *CSF1R* (c1061_1061 ins A), *KIT* (M541L), *PTEN* (c1373_1373 del A) and *PDGFRA* (E556V). In addition, there were four novel mutations identified; *TP53* (E154K, and D149E), *CSF1R* (c1061_1061 ins A) and *PDGFRA* (E556V). The pathogenicity prediction showed that only three mutations were pathogenic: *PTPN11* (E69K), *BRAF* (V600E) and *TP53* (E154K). These mutations result in changes of the proteins' structure and could affect their functions. Pathway analyses suggested that these genes are closely related to the pathogenesis of GBM through several pathways such as proliferation and invasion, metabolism and angiogenesis.

In conclusion, PGM in combination with the AmpliSeq Cancer Panel could be utilised as a potential molecular diagnostic tool not only for glioma but also for other cancers.

Introduction

Glioma is the most common form of primary brain tumours in adults and it could be highly malignant [1]. Glioma is characterised by diffused infiltration, increased angiogenesis, resistance to apoptosis, necrogenesis as well as genomic instability [1]. Traditionally, glioma is classified according to the World Health Organisation (WHO) grading scale, which was last revised in 2007 [2]. However, many histologically indistinguishable tumours exhibit their own discrete clinical course and outcome with similar treatment modality. Thus, prediction of prognosis and response to therapy may not be accurate based purely on histopathological classification [3]. Despite therapies such as surgical resection, radiotherapy and chemotherapy, the median survival of patients with glioma is between 12 – 15 months [4]. Hence, molecular genotyping is crucial in order to achieve reliable diagnostic and therapeutic improvement in

glioma patients [4]. Molecular genotyping would also be beneficial to both clinicians and patients in reducing the heterogeneous admixture and in focusing on accurately classified cases for targeted therapy using investigational new drugs based on their molecular signatures. Based on the molecular and genomic characterisation, glioma can be classified into low and high grade gliomas [5,6]. Low grade gliomas (I and II) are asymptomatic and grows slowly. In contrast, high grade glioma (III and IV) is the lethal type where tumour cells could diffuse into the normal cerebral cortex and could lead to death. The prognosis of the high grade glioma is poor compared to the low grade glioma. Several predictive markers have been identified for the diagnosis and prognostication of glioma and are currently on their way into clinical applications [4, 7-9]. For instance, tumours that harbor *IDH1* mutation are sensitive to temozolomide (TMZ) in low-grade glioma [10]. The *IDH1* is now used as a

diagnostic marker for diffuse grade I and III gliomas as well as secondary GBM, and the presence of mutation is associated with a better prognosis [4]. In addition, mutations in the mismatch repair gene (*MMR*) such as *MSH6* mediate TMZ resistance (11). Tumours with hypermethylation of the O-6 methylguanine-DNA-methyltransferase (*MGMT*) promoter may also develop resistance to TMZ therapy by gaining a hypermutator phenotype and mutations in the *MMR* gene [11]. However, combination between TMZ therapy and radiotherapy significantly increase the survival of patients' with methylated *MGMT* promoter when compared to patients who lacked *MGMT* promoter hypermethylation [12]. Rapid advancement in sequencing technologies have enabled researchers to perform whole-genome sequencing, targeted sequencing, and other applications using the next-generation sequencing [13]. Recently, several bench-top sequencing machines such as the Ion Torrent (Life Technologies, USA) or MiSeq (Illumina Inc., USA) have been launched to sequence small genomes such as bacteria genomes, as well as for targeted sequencing [14]. These NGS platforms allow mutational screening to be performed in a single day where a number of genes could be simultaneously sequenced with high accuracy [14]. The Ion Torrent Personal Genome Machine (PGM) in combination with the Ion AmpliSeq Cancer Panel are able to generate high-throughput screening of over 44 tumour suppressor genes and oncogenes which are frequently cited and mutated using a single-tube multiplex PCR assay with a small amount of starting DNA. Despite the knowledge and known mutations that have been detected in studies conducted in Western populations, the frequency and type of mutations in glioma patients from this region of the world has not been fully elucidated. Therefore, the aim of this study was to characterise the mutations involved in glioma patients in Malaysia population by using the PGM. The study may provide an insight into the pathogenesis of glioma in our population and could possibly be used for rapid molecular screening of glioma patients for a more detailed and accurate risk stratification.

Materials and methods

Patients and tumour specimens

All patients with primary brain tumour confirmed by diagnostic imaging techniques and underwent surgical excision at the Universiti Kebangsaan Malaysia Medical Centre (UKMMC) between the year 2010 and 2012 were included. Approval to conduct the research was obtained from the UKM Research Ethics Committee (UKM1.5.3.5/244/SPP/UMBI-001-2011). After informed consent, the demographic particulars and clinical data of the enrolled patients were

recorded. For each patient, a section of the tumour specimens was collected and snap-frozen in liquid nitrogen immediately upon tumour excision in the operating theatre. Histopathological examination (HPE) was performed by an experienced pathologist to exclude non-gliomas and to classify the glioma samples according to WHO grading. Specimens were also frozen-sectioned and H&E staining was performed for confirmation of 80% representation by another pathologist prior to DNA extraction. Tumour location was determined by magnetic resonance imaging (MRI) scan before surgery. In total, 16 glioma patients (grade I, II, III, and IV) were included in this study.

The demographic and clinical data of these patients are shown as in Table 1.

DNA isolation

DNA samples were isolated from 15mg tumour tissue using the QIAamp DNA Mini Kit (Qiagen, Germany). The quality and quantity of the DNA were determined using NanoDrop (Thermo Scientific, USA) and Qubit Fluorometric Quantitation, Double Stranded DNA Broad Range Assay kit (Invitrogen, USA) respectively. The DNA samples were diluted to 1.67 ng/ μ L for library preparation.

Library preparation

The AmpliSeq Cancer Panel which contains 190 primer pairs covering 44 common cancer-related genes was used for library amplification (Life Technologies, USA). The DNA was amplified using the 5X Ion AmpliSeqTM Primer Pool and the 5X Ion AmpliSeqTMHiFi Master Mix. The primers were partially digested using the FuPa reagent. Subsequently, adapters were ligated into the DNA sequences using the Switch solution, Ion AmpliSeq adapters, and DNA ligase. The samples were purified using Agent Court AMPure XP reagent (BD Biosciences, USA). The library was subjected to a second-round amplification using the Platinum PCR SuperMix High Fidelity, and Library Amplification Primer Mix. The amplified library was subjected to a two-round purification process using Agent Court AMPure XP reagent. Quantification of the library was performed on the AgilentTM Bioanalyzer instrument using the Agilent High Sensitivity DNA Kit (Agilent, Technologies, USA).

Template ion sphere particle (ISP) preparation using Ion One Touch System

The template ISP was prepared using the Ion One Touch Instrument. The Ion One TouchTM 200 Template kit protocol was utilized to prepare the

enriched template ISPs (Life Technologies, USA). Briefly, 10 - 20 pmol of the library was used to prepare the template ISP using the Ion One Touch™ 2X Reagent Mix, Enzyme Mix, and Ion One Touch Sphere Particles. Subsequently, the enriched template ISP was prepared using the Ion One Touch™ enrichment system. For quality control (QC), unenriched and enriched template ISPs was subjected to Qubit measurement to assess the polyclonal molecules. Only samples that passed the QC (% unenriched ISP <30% and % enriched template ISP >80%) were subjected to PGM sequencing.

PGM sequencing and data analysis

The sequencing run was performed according to the Ion Torrent PGM manual and the data generated were analysed using the Ion Torrent Suite software (Life Technologies, USA). The mutations were called using the Integrated Genome Variation software and confirmed with the SNPEFF software (<http://snpeff.sourceforge.net/download.html#install>). The patients' data were compared to the hg19 database.

Prediction of mutation pathogenicity

The Piezoelectric Micro Machine Ultrasonic Transducers (PMut) software which uses the neural network (NN) algorithm was applied to predict the pathogenicity of a particular mutation (<http://mmb2.pcb.ub.es:8080/PMut>) [15]. The neural network (NN) predicts the outcome of a particular mutation using different types of sequence information to label the mutations and subsequently process the information. A mutation is predicted to be pathogenic when the NN output is >0.5 [15].

Protein prediction tools

The protein sequence and transcripts for selected genes including *PTPN II*, *BRAF* and *TP53* were retrieved from NCBI database, UniPROT, and Protein Data Bank (PDB). The variant and functional effects were determined using the Variant Effect Predictor (<http://www.ensembl.org/info/docs/variation/vep/index.html>) [16], PolyPhen-2 (<http://genetics.bwh.harvard.edu/pph2/index.shtml>) [17], Basic Local Alignment Search Tool (BLAST) as well as SIFT (<http://sift.bii.a-star.edu.sg/>) [18] and SNAP (<http://sift.bii.a-star.edu.sg/>) softwares [19]. The protein stability was predicted using MuPro software (<http://mupro.proteomics.ics.uci.edu/>). The amino acid properties, protein function and structure as well as their 3D protein structure for mutated gene were analysed (please change all to UK spelling) using

Project HOPE web based tool (<http://www.cmbi.ru.nl/hope/home>).

Validation using Sanger sequencing

Samples with mutations were validated using the Sanger sequencing method. Primers from the AmpliSeq Cancer Panel for the selected validation were used for Sanger sequencing. Briefly, PCR products were generated and cycle sequencing was performed using the Big Dye Terminator V3.1 reagent (Life Technologies, USA). The cycle sequencing products were then processed using ethanol precipitation and sequencing was carried out using the ABI 3100 capillary electrophoresis (Life Technologies, USA). The results were analysed using Basic Local Alignment System Tool (BLAST). New primers were designed for the validation in cases where we failed to amplify or sequence using primers from the AmpliSeq Cancer Panel.

Validation using TaqMan® Mutation Assay

The small deletion and insertion in the *PTEN* and *CSFRI* were validated using Custom TaqMan® Mutation Assay. The assay was performed according to the protocol described by the manufacturer (Life Technologies, USA). Mutation was detected using allelic discrimination assay analysis.

Results

In total, 16 glioma patients were included in this study (four patients for each grade). The patients' age ranged between four to 64 years old. 14 patients were males, and two were females. Seven patients were Chinese whereas nine were Malays. Tumour location and the HPE descriptions for these patients are indicated in Table 1. Most of the patients are still alive and only three patients have died due to the disease. The survival of three patients could not be retrieved due to default follow-up.

Table 2 shows the data generated using the Torrent Suite software. The number of bases (Mbp) generated range between 27.91 Mbp and 47.82 Mbp, which is above the detection limit. The identified mutations are listed in Table 3. A total of 14 mutations were identified and these included 12 missense mutations in *KDR*, *MLH1*, *MET*, *PTPN11*, *PDGFRA*, *BRAF*, *IDH1*, *PIK3CA*, *KIT*, and *TP53* (3 mutations). Two frameshift mutations were detected in the *CSFIR* (c1061_1061 ins A) and *PTEN* (c1373_1373 del A) genes. Most of the samples carry more than one mutations. These mutations were compared to the Catalogue of Somatic Mutations in Cancer (COSMIC) in order to search for novel mutations. Four mutations

were confirmed to be novel, which included E154K and D149E in *TP53*, the frameshift mutation in *CSF1R*

Table 1: Demographic and clinical data of glioma patients involved in the study

WHO Grade	Sample ID	Age at diagnosis (Years)	Age at specimen collection (Years)	Gender	Ethnic	New case	Tumour location	Survival (Months)	HPE description
1	BT21	4	4	F	MY	Yes	Suprasellar	Alive	Pilocytic astrocytoma
	BT49	33	33	M	MY	Yes	Suprasellar	Alive	Pilocytic astrocytoma
	BT54	18	27	M	CH	No	Left optic nerve	Alive	Pilocytic astrocytoma
	BT94	1	1	M	MY	Yes	Right frontal parasagittal	Alive	Desmoplastic infantile astrocytoma
2	BT31	40	40	M	MY	Yes	Deep left frontal	Alive	Firillary astrocytoma
	BT40	30	40	M	MY	No	Right frontal	N/A	Oligodendroglioma
	BT69	23	41	M	MY	No	Right lateral ventricular	Alive	Ependymoma
	BT98	15	22	M	MY	No	Left parietal	Alive	Pleomorphic xanthomatous astrocytoma
3	BT7	10	10	M	CH	Yes	Left basal ganglia	1	Anaplastic glioma with clear cell ependymoma
	BT63	26	31	M	MY	No	Left frontal	Alive	Anaplastic oligodendroglioma
	BT74	14	14	M	MY	Yes	Third ventricular	Alive	Anaplastic ependymoma
	BT108	42	42	M	CH	Yes	Deep bifrontal	Alive	Anaplastic oligodendroglioma
4	BT2	58	58	M	CH	Yes	Deep left parietal	0.3	Glioblastomamultiforme
	BT4	57	57	F	CH	Yes	Left temporal	N/A	Gliosarcoma
	BT8	61	61	M	CH	No	Right temporal	8.5	Glioblastomamultiforme
	BT10	64	64	M	CH	Yes	Left temporo-occipital	N/A	Glioblastomamultiforme

*(F: Female; M: Male; MY: Malay; CH: Chinese; N/A: Not available (Default follow up); HPE: Histopathological Examination)

Table 2: Data generated from the Personal Genome Machine sequencing of glioma patients

No	Samples	Total number of bases (Mbp)	No of Q20 bases (Mbp)	Total no of reads	Mean length (bp)	Longest read (bp)
1	21T_GI	35.21	32.65	427,573	82	203
2	49T_GI	47.43	44.1	581,998	82	198
3	54T_GI	37.54	35.28	481,598	78	201
4	94T_GI	45.02	40.88	562,787	80	202
5	31T_GII	34.15	31.59	426,942	80	202
6	40T_GII	27.19	24.67	340,375	80	202
7	69T_GII	37.99	34.53	476,121	80	200
8	98T_GII	46.52	43.28	576,446	81	202
9	63T_GIII	47.82	43.43	588,755	81	201
10	74T_GIII	38.31	34.79	478,196	80	202
11	108T_GIII	44.29	41.33	547,250	81	202
12	7T_GIII	45.57	42.06	501,388	91	202
13	10T_GIV	37.98	32	500,490	76	196
14	2T_GIV	43.91	40.45	552,828	79	203
15	4T_GIV	45.04	41.32	560,437	80	202
16	8T_GIV	41.09	43.28	576,446	81	202

Table 3: Mutations identified in the glioma patients using the Personal Genome Machine

No	Samples	Chrom	Position	Gene	Type	Ploidy	Ref	Var	Acid Amino changes	Exon	Variant Coverage	HotSpotID
1	21T_GI	4	55972974	<i>KDR</i>	SNP	Het	T	A	Q472H	11	1488	COSM149673
		3	37067240	<i>MLH1</i>	SNP	Het	T	A	V384D	12	1545	COSM26085
2	54T_GI	4	55972974	<i>KDR</i>	SNP	Het	T	A	Q472H	11	2041	COSM149673
		7	116340262	<i>MET</i>	SNP	Het	A	G	N375S	2	1571	COSM710
		12	112888189	<i>PTPN11</i>	SNP	Het	G	A	E69K	3	2965	COSM13013
3	31T_GII	7	140453136	<i>BRAF</i>	SNP	Het	A	T	V600E	15	2918	COSM149673
		17	7577082	<i>TP53</i>	SNP	Het	C	T	E154K	4	2852	-
		2	209113112	<i>IDH1</i>	SNP	Het	C	T	R132H	4	1523	COSM28746
4	40T_GII	3	178952085	<i>PIK3CA</i>	SNP	Het	A	G	H1047R	21	3975	COSM775,
		4	55972974	<i>KDR</i>	SNP	Het	T	A	Q472H	11	932	COSM149673
		5	149453048	<i>CSF1R</i>	INS	Het	A	AA	Frameshift	7	1603	-
5	69T_GII	4	55972974	<i>KDR</i>	SNP	Het	T	A	Q472H	11	2008	COSM149673
		4	55593464	<i>KIT</i>	SNP	Het	A	C	M541L	10	846	COSM28026
6	98T_GII	4	55972974	<i>KDR</i>	SNP	Het	T	A	Q472H	11	1034	COSM149673
		7	140453136	<i>BRAF</i>	SNP	Het	A	T	V600E	15	1080	COSM476,
7	7T_GIII	10	89624242	<i>PTEN</i>	DEL	Hom	AA	A	Frameshift	1	73	COSM4937; COSM4929
8	63T_GIII	4	55972974	<i>KDR</i>	SNP	Hom	T	A	Q472H	11	1352	COSM149673
		5	149453048	<i>CSF1R</i>	INS	Het	A	AA	Frameshift	7	1302	-
		7	116340262	<i>MET</i>	SNP	Hom	A	G	N375S	2	5267	COSM710
9	74T_GIII	4	55972974	<i>KDR</i>	SNP	Hom	T	A	Q472H	11	2196	COSM149673
		5	149453048	<i>CSF1R</i>	INS	Het	A	AA	Frameshift	7	470	-
10	108_GIII	4	55972974	<i>KDR</i>	SNP	Hom	T	A	Q472H	11	1892	COSM149673
		17	7578461	<i>TP53</i>	SNP	Het	C	A	V157F	4	1199	COSM10670
11	108_GIII	4	55972974	<i>KDR</i>	SNP	Hom	T	A	Q472H	11	1892	COSM149673
12	2T_GIV	4	55972974	<i>KDR</i>	SNP	Hom	T	A	Q472H	11	981	COSM149673
		7	140453136	<i>BRAF</i>	SNP	Het	A	T	V600E	15	2565	COSM476
13	8T_GIV	17	7577082	<i>TP53</i>	SNP	Het	C	T	E154K	4	2482	-
		3	178952085	<i>PIK3CA</i>	SNP	Het	A	G	H1047R	21	2386	COSM775
		4	551412021	<i>PDGFRA</i>	SNP	Het	A	T	E556V	12	1579	-
13	10T_GIV	4	55972974	<i>KDR</i>	SNP	Het	T	A	Q472H	11	1146	COSM149673
		17	7577095	<i>TP53</i>	SNP	Het	G	C	D149E	4	3445	-

(Chrom: Chromosome, Ref: Reference, Var: Variant)

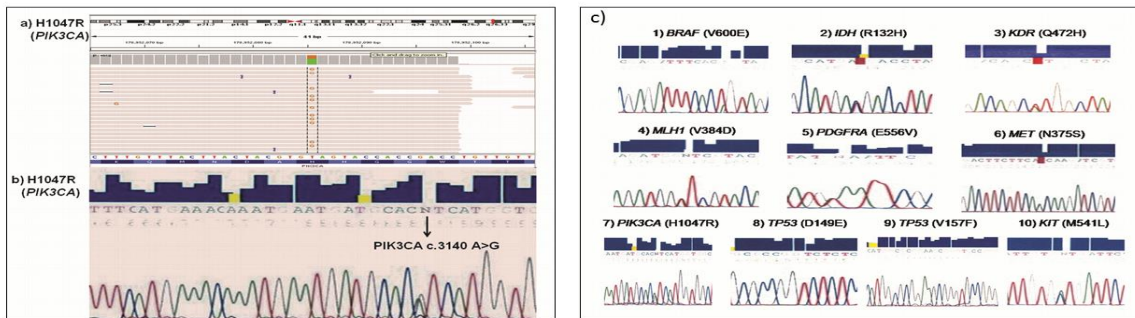


Figure 1

a,b) The H1047R mutation in the PIK3CA gene in a patient with grade IV glioma. This mutation involved a nucleotide change from A>G at position 3140 of the gene which was detected by PGM. c) The result was validated using Sanger sequencing which confirmed the mutation, PIK3CA c.3140 A>G in this patient.

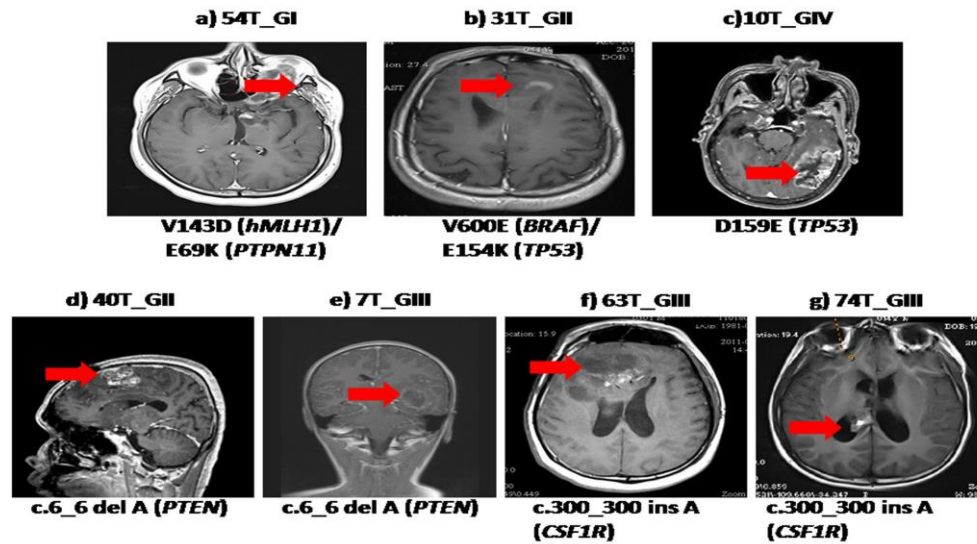


Figure 2

MRI scan images of selected samples with their corresponding sequencing results. (a) A recurrent pilocytic astrocytoma of the left optic nerve in which the tumour bulk (arrow) occupied the whole retro-orbital region. (b) Minimal enhancement seen in a post-gadolinium contrasted MRI image of a left frontal fibrillary astrocytoma lesion (arrow). (c) A large heterogeneous lesion with central necrotic area (arrow) seen in the left temporo-occipital region of a newly diagnosed GBM. (d) A recurrent right frontal oligodendroglioma (arrow). (e) Grade 3 anaplastic glioma with clear cell ependymoma was confirmed from the tumour sample excised from the left basal ganglia (arrow). (f) Huge recurrent left frontal anaplastic oligodendroglioma (WHO grade 3) (arrow) was seen impinging the lateral ventricles. (g) Lesion at right ventricle with increased signal intensity (arrow) of patient 74T was confirmed as grade 3 anaplastic ependymoma. It was not possible to correlate between the genotype and phenotype since the number of samples is too small.

and E556V in *PDGFRA*. Two patients with Grade I glioma showed mutations in *KDR*, *MLH1*, *MET*, and *PTPN11*. Mutations in *BRAF*, *TP53*, *IDH1*, *PIK3CA*, *KDR* and *KIT* genes were identified in those with Grade II gliomas. In addition, an insertion of A at position 149453048 of chromosome 5 of the *CSF1R* (c1061_1061 ins A) gene was identified in one patient. For the Grade III patients, four missense mutations were identified in the *KDR*, *CSF1R*, *MET*, and *TP53* genes. A frameshift mutation in the *PTEN* (c1371_1373 del A) gene was also identified in another patient. Six missense mutations were detected in *KDR* and *BRAF*, 2 in *TP53*, *PIK3CA*, and *PDGFRA* in the Grade IV glioma patients. The H1047R mutation in the *PIK3CA* gene in a patient with grade IV glioma involved a nucleotide change from A>G at position 3140 of the gene which was detected by PGM (Table 1a, b).

In total, three mutations were predicted to be pathogenic. These are the mutations in *PTPN11* (E69K, NN: 0.6476), *BRAF* (V600E, NN:0.8083), and *TP53* (E154K, NN:0.6886). The effects of these mutations on the protein functions were predicted

using PolyPhen-2 software. It showed that these mutations might lead to protein damage with scores of 0.970, 0.971, and 0.996 respectively. Mutations in the *MLH1*, *MET*, *KDR*, *KIT*, *TP53* (D149E and V157F), *IDH1*, *PIK3CA*, and *PDGFRA* were validated using Sanger sequencing (Figure 1c). However, Sanger sequencing is not sensitive to detect mutations with reduced frequency of mutant alleles. Mutation in the *PTPN11* and *TP53* (E154K), could not be detected using this technique. The mutant allele's frequency in the *PTPN11* was 9%, and samples with *TP53* (E154K) mutations showed 24 to 26%.

PTEN deletion could not be validated using the Taqman[®] Mutation Detection Assay due to low variant coverage which is 73. We also failed to validate the *CSF1R* insertion using this technique despite the high variant coverage which is between 470-1603. MRI scan images of selected samples with their corresponding sequencing results were shown as in Figure 2.

Discussion

The Sanger sequencing approach has been employed for more than 30 years to detect mutations in many diseases including cancers [20,21]. Nevertheless, the Sanger method is time consuming and multiple genes cannot be sequenced simultaneously. Cancer is a complex disease that involves multiple gene rearrangements and mutations.

Therefore, the third-generation sequencing platform could be the method of choice for mutational screening in cancers due to its capability to sequence multiple genes simultaneously and less time consuming [14]. We employed the Ion Torrent Personal Genome Machine (PGM) in combination with the Ion AmpliSeq Cancer Panel to analyse 16 gliomas from different grades and identified a total of 14 mutations. The *KDR* gene mutation (Q472H) was observed in all glioma grades and ten out of the 16 patients harbor this mutation. The *KDR* or *VEGF* gene is a major growth factor for endothelial cells and plays a role in angiogenesis, vascular development, vascular permeability, and embryonic hematopoiesis [22]. Given that *VEGF* is a pro-angiogenesis factor hence a crucial role in pathogenicity and metastasis [23], this mutation was expected to be seen more frequently in the high grade compared to the low grade gliomas. However, the occurrence of the *KDR* mutation as the sole mutation was seen in all grades i.e. in GI (21T_GI), GII (69T_GII), GIII (108_GIII), and GIV (2T_GIV) patients. In addition, a GIII glioma patient (7T_GIII) had only *PTEN* mutation. These solitary mutations may not be the direct cause of glioma in these patients as cancer is a multistep process that involves multiple genes abnormalities. The hotspot cancer panel that we used in this study only contain 44 cancer-related genes. Thus, we could not exclude the possibility that there are other key genes that involved in the pathogenesis of glioma that are not represented in this panel. The heterogeneity and the diffusive nature of glioma cells possess a great challenge in order to extract pure biology molecules without being contaminated by normal or stromal tissues. Here, we performed frozen sections for confirmation of the tumour resection. Only patients with 80% tumour cells were enrolled in this study to ensure representative of cancer tissues.

The *TP53* gene is essential for the metabolic and angiogenesis processes in the glioma tumourigenesis [24-25]. Three mutations (D149E, E154K, and V157F) in the *TP53* gene were identified, of which 2 were novel mutations (D149E and E154K). However, only the E154K mutation was pathogenic with an NN output of 0.7171. This mutation is located within the domain that is crucial for *TP53* activity, which includes interaction with *HIPK1*, *AXINI*, and *E4F1*. The mutant residue may affect the protein function in

several ways. First, the mutant residue leads to changes in the protein charge, which subsequently could cause repulsion between residues in the protein core. Additionally, this could also interrupt the ionic interaction between the residues in the protein core, reducing the catalytic activity of the protein. Second, the mutant residue may differ in size when compared to the wild-type sequence causing it to reside incorrectly in the core protein. Consequently, a different hydrogen bond will be made as a result of the incorrect position of the mutant residue. Both aspects may diminish the interaction with key proteins involved in *TP53* functions. The patient (31T_GII) who carried this mutation is a Malay male aged 40 years, and had a fibrillary astrocytoma located at the deep left frontal lobe. We also detected the *BRAF* (V600E, pathogenic) mutation in this patient who is still alive after a year of diagnosis. In contrast, a Chinese patient aged 61 years with GBM at the right temporal lobe (8T_GIV) also had *TP53* (E154K) and *BRAF* (V600E) mutations but died after 8.5 months of diagnosis. Although both patients carried the same mutations, the type of glioma is most likely to determine the survival rate of the patients. Another patient (98T_GII) who had mutations in *BRAF* (V600E), *KIT* (M541L) and *KDR* (Q472H) genes is still surviving seven years after being diagnosed with pleomorphic xanthomatous astrocytoma (PXA). In comparison, one patient with type IV glioma (2T_GIV) who carried the non-pathogenic *KDR* (Q472H) mutation died at 0.3 months following diagnosis of GBM at the deep left parietal lobe of the brain. There was no other mutation identified in this patient. The patient (7T_GIII) with a frameshift mutation (c1373_1373 del A) in the *PTEN* gene died at the age of ten years, one month after being diagnosed with glioma at the left basal ganglia of the brain. *PTEN* is a tumour suppressor gene and is involved in modulating cell cycle progression and cell survival by the PI3K-AKT/PKB signaling pathway. The sample size is rather small to perform a genotype-based correlation analysis with outcome. Also the difficulty in getting normal brain samples as a comparison.

The frameshift mutation in the *CSF1R* gene, which is also a novel mutation, was identified in two patients, one with Grade II and another with Grade III glioma. *CSF1R* is a cytokine that controls the production and differentiation of macrophages hence is not related to the pathway involved in glioma. The E556V mutation in the *PDGFRA* gene is also a novel mutation that was identified in a patient with GIV glioma. *PDGFRA* is a transmembrane protein that consists of 5 immunoglobulin-like repeats in the extracellular domain and intracellular tyrosine-kinase domain [26]. Activation of the *PDGFRA* receptor by its ligand results in signal transduction of the downstream

pathways such as MAP kinase, PI3-kinase/AKT and JAK/STAT1 [26]. These pathways play a major role in cellular proliferation, differentiation, invasion, and survival. The patient (10T_GIV) is a Chinese man, aged 64 years with GBM at the left temporo-occipital lobe of the brain. We could not retrieve the survival rate of this patient as he had defaulted follow-up.

A missense mutation was identified in the *MLH1* gene (V384D) in one of the grade I glioma patients (54T_GI, 27 years old). *MLH1* mutations have been shown to be strongly associated with inherited Lynch syndrome and also Turcot syndrome [27]. Deimling and colleagues performed sequencing of exon 15 of the *BRAF* gene on 1320 brain tumours and found that 93 out of 96 mutations detected were of the V600E-type [28]. The study reported that 66% of the *BRAF* V600E variant was found in grade II pleomorphic xanthoastrocytomas (PXA). One other study detected *BRAF* V600E mutation in 12 out of 20 (60%) patients with WHO Grade II PXA [29]. In our study, two out of four patients (50%) with grade II tumours harbored the *BRAF* V600E variant. The studies on the *BRAF* V600E variant have shown that this mutation could be a promising molecular biomarker and could also be potentially targeted for therapy [29].

Mutation in the *PIK3CA* gene has been shown to be associated with GBM, oligodendrogliomas, and several other brain tumour types [30,31]. Two patients were identified with *PIK3CA* (H1047R) variant i.e. one with oligodendroglioma (40T_GII) and the other with GBM (10T_GIV). High frequency of the *IDH1* (R132H) variant (66-100%) was present in oligodendrogliomas and oligoastrocytomas in several populations such as in Germany and USA [32-35]. A specific antibody against this variant has been developed hence *IDH1* could be a reliable diagnostic tool to distinguish between these types of brain tumour from the other forms [36]. However, the frequency of this mutation in our population is low (1/16) patients compared to other populations. It is noted that mutations in the *RBI* gene was absent in all patients studied. This could be due to the cancer panel only focuses on nine common mutations in the *RBI* gene. Further mutational analysis in genes commonly involved in glioma can be performed using target-resequencing or whole exome sequencing. We compared our results with The Cancer Genome Atlas (TCGA) to observe whether there are similarities or differences between our glioma patients and TCGA samples [37]. Mutation Significance (MutSig) has identified 8 significant genes that involve in glioblastoma which are *TP53*, *PTEN*, *ERBB2*, *PIK3R1*, *NF1*, *EGFR*, *RBI* and *PIK3CA*. Out of these eight significant genes, only mutations in *PTEN*, *TP53* and *PIK3CA* were observed in our study. We identified ten genes in our cohort study and from these ten genes, only six genes were in concordance with the

TCGA database; *MLH1*, *MET*, *PTPN11*, *TP53*, *PIK3CA* and *PDGFRA*. Nevertheless, most of the identified mutations differ from the TCGA database in term of the types and positions, except for the E69K mutation in the *PTPN11*. This suggests that the potential causes of glioma in Malaysian population could be contributed by different genetic alterations compared to the Caucasian population. However, these observations need to be verified in a larger sample size (n = 206 in TCGA).

In total, ten missense mutations were validated using Sanger sequencing. Two mutations [*PTPN11* (E69K) and *TP53* (E154K)] could not be detected using Sanger sequencing due to the low frequency of the mutated alleles (E69K with a mutant allele frequency of 9% and E154K with a mutant frequency of 24%-26%). We designed a probe for the TaqMan[®] Mutation Detection Assay based on the small deletion and insertion detected by the Ion Torrent. For *PTEN* A deletion, the result showed that there was no deletion and the gene was homozygous wild type. Subsequently, we did Sanger sequencing to further confirm this mutation and we detected the AA deletion instead of the A deletion. Sanger sequencing or TaqMan[®] Mutation Detection Assay may not be sufficient to validate the presence of the mutated alleles that exist in low copy number (variant coverage = 73, Table 3). Therefore, in order to correctly validate these mutated alleles, copy number variation experiment needs to be conducted to fulfill the given validation process. We also could not validate the *CSF1R* A insertion using both Sanger sequencing and TaqMan[®] Mutation Detection Assay although the variant coverage of mutant and wild type is about 50%. Other sequencing platforms such as MiSeq or NextSeq could be used in order to validate this mutation.

Conclusion

In conclusion, we have successfully identified 14 mutations (four novel and three pathogenic) in 16 glioma samples by utilizing the PGM platform. The *KDR* gene mutation was the most common alteration and was present in all grades in our cohort of patients. PGM has opened a new era in mutation screening since it offers a robust and faster method for sequencing analysis. In conclusion, PGM in combination with the AmpliSeq Cancer Panel could potentially offer a better molecular diagnosis for glioma and any other cancers.

Acknowledgement

We would like to thank Janice Khor Sheau Sean and Alex Teoh View Hune from Analisa Resources (M) Sdn. Bhd. for their contribution. This study was

supported by the UKMMC Genomic Unit-UKM UMBI and the Higher Institution Centre of Excellent (HiCOE) grant, Ministry of Higher Education, Malaysia.

References

- Bonavia R, Inda MM, Cavenee WK, Furnari FB. Heterogeneity maintenance in glioblastoma: a social network. *Cancer Res* 2011, 71(12):4055-60.
- Louis DN OH, Wiestler OD, Cavenee WK. *WHO Classification of tumours of the central nervous system*. 3rd edition ed. Lyon: IARC Press; 2007.
- Matthews S, Succar P, Jelinek H, McParland B, Buckland M, McLachlan CS. Diagnosis of oligodendroglioma: molecular and classical histological assessment in the twenty-first century. *Asia Pac J Clin Oncol* 2012, 8(3):213-6.
- Riemenschneider MJ, Reifenberger G. Molecular neuropathology of gliomas. *Int J Mol Sci* 2009, 10(1):184-212.
- Gladson CL, Prayson RA, Liu WM. The pathobiology of glioma tumours. *Annu Rev Pathol* 2010, 5:33-50.
- Burgess R, Jenkins R, Zhang Z. Epigenetic changes in gliomas. *Cancer Biol Ther* 2008, 7(9):1326-34.
- Nicolaidis S. Personalized medicine in neurosurgery. *Metabolism* 2012, 62 (Suppl 1):S45-8.
- Mukasa A, Takayanagi S, Saito K, Shibahara J, Tabei Y, Furuya K, Ide T, Narita Y, Nishikawa R, Ueki K, Saito NI. Significance of IDH mutations varies with tumour histology, grade, and genetics in Japanese glioma patients. *Cancer Sci* 2012, 103(3):587-92.
- Yan W, Zhang W, You G, Bao Z, Wang Y, Liu Y, Kang C, You Y, Wang L, Jiang T. Correlation of IDH1 mutation with clinicopathologic factors and prognosis in primary glioblastoma: a report of 118 patients from China. *PLoS One* 2012, 7(1):e30339.
- Houillier C, Wang X, Kaloshi G, Mokhtari K, Guillemin R, Laffaire J, Paris S, Boisselier B, Idbaih A, Laigle-Donadey F, Hoang-Xuan K, Sanson M, Delattre JY. IDH1 or IDH2 mutations predict longer survival and response to temozolomide in low-grade gliomas. *Neurology* 2010, 75(17):1560-6.
- Cancer Genome Atlas Network. Comprehensive molecular characterization of human colon and rectal cancer. *Nature* 2012, 487(7407):330-7.
- Hegi ME, Diserens AC, Gorlia T, Hamou MF, de Tribolet N, Weller M, Kros JM, Hainfellner JA, Mason W, Mariani L, Bromberg JE, Hau P, Mirimanoff RO, Cairncross JG, Janzer RC, Stupp R. MGMT gene silencing and benefit from temozolomide in glioblastoma. *N Engl J Med* 2005, 352(10):997-1003.
- Elliott AM, Radecki J, Moghis B, Li X, Kammesheidt A. Rapid detection of the ACMG/ACOG-recommended 23 CFTR disease-causing mutations using ion torrent semiconductor sequencing. *J Biomol Tech* 2012, 23(1):24-30.
- Chan M, Ji SM, Yeo ZX, Gan L, Yap E, Yap YS, Ng R, Tan PH, Ho GH, Ang P, Lee AS. Development of a Next-Generation Sequencing Method for BRCA Mutation Screening: A Comparison between a High-Throughput and a Benchtop Platform. *J Mol Diagn* 2012, 14(6):602-12.
- Ferrer-Costa C, Gelpi JL, Zamakola L, Parraga I, de la Cruz X, Orozco M. PMUT: a web-based tool for the annotation of pathological mutations on proteins. *Bioinformatics* 2005, 21(14):3176-8.
- McLaren W, Pritchard B, Rios D, Chen Y, Flicek P, Cunningham F. Deriving the consequences of genomic variants with the Ensembl API and SNP Effect Predictor. *Bioinformatics* 2010, 26(16):2069-70.
- Adzhubei IA, Schmidt S, Peshkin L, Ramensky VE, Gerasimova A, Bork P, Kondrashov AS, Sunyaev SR. A method and server for predicting damaging missense mutations. *Nat Methods* 2010, 7(4):248-9.
- Altschul SF, Gish W, Miller W, Myers EW, Lipman DJ. Basic local alignment search tool. *J Mol Biol* 1990, 215(3):403-10.
- Bromberg Y, Rost B. SNAP: predict effect of non-synonymous polymorphisms on function. *Nucleic Acids Res* 2007, 35(11):3823-35.
- Abdul Murad NA, Othman Z, Khalid M, Abdul Razak Z, Hussain R, Nadesan S, Sagap I, Mohamed Rose I, Wan Ngah WZ, Jamal R. Missense Mutations in MLH1, MSH2, KRAS, and APC Genes in Colorectal Cancer Patients in Malaysia. *Dig Dis Sci* 2012, 57(11):2863-72.
- Azian M, Hapizah MN, Khalid BA, Khalid Y, Rosli A, Jamal R. Use of the denaturing gradient gel electrophoresis (DGGE) method for mutational screening of patients with familial hypercholesterolaemia (FH) and Familial defective apolipoprotein B100 (FDB). *Malays J Pathol* 2006, 28(1):7-15.
- Cudmore MJ, Hewett PW, Ahmad S, Wang KQ, Cai M, Al-Ani B, Fujisawa T, Ma B, Sissaoui S, Ramma W, Miller MR, Newby DE, Gu Y, Barleon B, Weich H, Ahmed A. The role of heterodimerization between VEGFR-1 and VEGFR-2 in the regulation of endothelial cell homeostasis. *Nat Commun* 2012, 3:972.
- Patel M, Vogelbaum MA, Barnett GH, Jalali R, Ahluwalia MS. Molecular targeted therapy in

- recurrent glioblastoma: current challenges and future directions. *Expert Opin Investig Drugs* 2012, 21(9):1247-66.
24. Egan KM, Nabors LB, Olson JJ, Monteiro AN, Browning JE, Madden MH, Thompson RC. Rare TP53 genetic variant associated with glioma risk and outcome. *J Med Genet* 2012, 49(7):420-1.
 25. Suh SS, Yoo JY, Nuovo GJ, Jeon YJ, Kim S, Lee TJ, Kim T, Bakacs A, Alder H, Kaur B, Ageilan RI, Pichiorri F, Croce CM. MicroRNAs/TP53 feedback circuitry in glioblastoma multiforme. *Proc Natl Acad Sci U S A* 2012, 109(14):5316-21.
 26. Reis RM, Martins A, Ribeiro SA, Basto D, Longatto-Filho A, Schmitt FC, Lopes JM. Molecular characterization of PDGFR-alpha/PDGF-A and c-KIT/SCF in gliosarcomas. *Cell Oncol* 2005, 27(5-6):319-26.
 27. Lebrun C, Olschwang S, Jeannin S, Vandenbos F, Sobol H, Frenay M. Turcot syndrome confirmed with molecular analysis. *Eur J Neurol* 2007, 14(4):470-2.
 28. Schindler G, Capper D, Meyer J, Janzarik W, Omran H, Herold-Mende C, Schmieder K, Wesseling P, Mawrin C, Hasselblatt M, Louis DN, Korshunov A, Pfister S, Hartmann C, Paulus W, Reifenberger G, von Deimling A. Analysis of BRAF V600E mutation in 1,320 nervous system tumours reveals high mutation frequencies in pleomorphic xanthoastrocytoma, ganglioglioma and extra-cerebellar pilocytic astrocytoma. *Acta Neuropathol* 2011, 121(3):397-405.
 29. Dias-Santagata D, Lam Q, Vernovsky K, Vena N, Lennerz JK, Borger DR, Batchelor TT, Ligon KL, Lafrate AJ, Ligon AH, Louis DN, Santagata S. BRAF V600E mutations are common in pleomorphic xanthoastrocytoma: diagnostic and therapeutic implications. *PLoS One* 2011, 6(3):e17948.
 30. Broderick DK, Di C, Parrett TJ, Samuels YR, Cummins JM, McLendon RE, Fults DW, Velculescu VE, Bigner DD, Yan H. Mutations of PIK3CA in anaplastic oligodendrogliomas, high-grade astrocytomas, and medulloblastomas. *Cancer Res* 2004, 64(15):5048-50.
 31. Gallia GL, Rand V, Siu IM, Eberhart CG, James CD, Marie SK, Oba-Shinjo SM, Carlotti CG, Caballero OL, Simpson AJ, Brock MV, Massion PP, Carson BS Sr, Riggins GJ. PIK3CA gene mutations in pediatric and adult glioblastoma multiforme. *Mol Cancer Res* 2006, 4(10):709-14.
 32. Bals J, Meyer J, Mueller W, Korshunov A, Hartmann C, von Deimling A. Analysis of the IDH1 codon 132 mutation in brain tumours. *Acta Neuropathol* 2008, 116(6):597-602.
 33. Hartmann C, Meyer J, Bals J, Capper D, Mueller W, Christians A, Felsberg J, Wolter M, Mawrin C, Wick W, Weller M, Herold-Mende C, Unterberg A, Jeuken JW, Wesseling P, Reifenberger G, von Deimling A. Type and frequency of IDH1 and IDH2 mutations are related to astrocytic and oligodendroglial differentiation and age: a study of 1,010 diffuse gliomas. *Acta Neuropathol* 2009, 118(4):469-74.
 34. Watanabe T, Nobusawa S, Kleihues P, Ohgaki H. IDH1 mutations are early events in the development of astrocytomas and oligodendrogliomas. *Am J Pathol* 2009, 174(4):1149-53.
 35. Yan H, Parsons DW, Jin G, McLendon R, Rasheed BA, Yuan W, Kos I, Batinic-Haberle I, Jones S, Riggins GJ, Friedman H, Reardon D, Herndon J, Kinzler KW, Velculescu VE, Vogelstein B, Bigner DD. IDH1 and IDH2 mutations in gliomas. *N Engl J Med* 2009, 360(8):765-73.
 36. Capper D, Reuss D, Schittenhelm J, Hartmann C, Bremer J, Sahm F, Harter PN, Jeibmann A, von Deimling A. Mutation-specific IDH1 antibody differentiates oligodendrogliomas and oligoastrocytomas from other brain tumours with oligodendrogloma-like morphology. *Acta Neuropathol* 2011, 121(2):2